# Induction of Circular Dichroism by Coadsorption of Chiral and Achiral Metal Complexes on a Colloidal Clay

**Kazunari Naka,[†] Hisako Sato,[‡,§] Taketoshi Fujita,[⊥] Nobuo Iyi,[⊥] and Akihiko Yamagishi*[,‡,§]**

*Department of Chemistry, Graduate School of Science, Hiroshima University, Kagamiyama 1-3-1, Higasi-Hiroshima 739-8526, Japan, Graduate School of Science, Department of Earth and Planetary Science, The University of Tokyo, Hongo, Tokyo 113-0033, Japan, CREST, Japan Science and Technology Corporation, Japan, and Aist, Tsukuba, Ibaraki 305-8561, Japan*

*Received: November 12, 2002; In Final Form: April 25, 2003*

Two kinds of metal complexes, an achiral metal complex, $[Fe(terpy)]^{2+}$ (terpy = 2,2′,2″-terpyridyl), and a chiral metal complex, $\Delta$-$[Ni(phen)_3]^{2+}$ (phen = 1,10-phenanthroline), were coadsorbed by colloidally dispersed sodium saponite clay. Interaction between these molecules on a clay surface was investigated by electric dichroism and circular dichroism measurements. The molecular orientation of an adsorbed $[Fe(terpy)]^{2+}$ ion was determined in the absence or presence of $\Delta$-$[Ni(phen)_3]^{2+}$ by electric dichroism measurements. The angle of the $C_2$ axis of $[Fe(terpy)]^{2+}$ with respect to a clay surface changed from 35.4° to 44.4° when the complex was coadsorbed with $\Delta$-$[Ni(phen)_3]^{2+}$. The circular dichroism spectrum of a clay dispersion containing $[Fe(terpy)]Cl_2$ and $\Delta$-$[Ni(phen)_3]Cl_2$ was measured in the wavelength region of 350−600 nm. $\Delta$-$[Ni(phen)_3]^{2+}$ had no electronic absorption in this region. Circular dichroism due to adsorbed $[Fe(terpy)]^{2+}$ appeared when $\Delta$-$[Ni(phen)_3]Cl_2$ was added to the ratio of $[Fe(terpy)]Cl_2/\Delta$-$[Ni(phen)_3]Cl_2$ from 1:1 to 1:3. The results were compared with the prediction by Kirkwood−Tinoco theory, in which circular dichroism is assumed to be induced by dipolar interaction with a chiral molecule.

## Introduction

A smectite-type clay mineral is a layered phyllosilicate in which the octahedral sheet of aluminum or magnesium oxides is sandwiched by two tetrahedral sheets of silicates.[1] It is characterized by submicron particle size, cation-exchange capability, and swelling properties. Its extremely flat morphology of an external layer surface or in an interlayer space provides an interesting heterogeneous medium for chemical reactions. In particular, molecular discrimination among coadsorbed molecules has been one of the most attracting aspects in the reactions involving these clay minerals.[2−3]

We have been presenting examples for the enhancement of chirality recognition by adsorbed metal complexes on a clay surface.[4−6] On a clay surface, a chiral metal complex such as tris(1,10-phananthroline)metal(II) ($[M(phen)_3]^{2+}$), for example, has been proven to interact with organic and inorganic molecules in a stereoselective way. Such high sensitivity toward molecular chirality is difficult to be realized on other kinds of ion exchangers such as ion-exchanging resins or layered metal oxides. The network structure of a silicate sheet is believed to be a main factor to achieve the uniform orientation and regular arrangement of adsorbed $[M(phen)_3]^{2+}$ molecules.[7−9]

One of the key aspects to understanding molecular discrimination on a clay surface is to reveal the detailed mechanism of intermolecular interaction among adsorbed molecules. For those purposes, many kinds of spectroscopic methods have been applied such as X-ray diffraction analyses, FT-IR spectra, UV−vis absorption, steady-state and transient fluorescence measurements, and magnetic resonance spectroscopy.[10] In the present work, we report the detailed analyses of induced circular dichroism of an achiral metal complex that is coadsorbed with a chiral metal complex. Chirality in the electronic absorption spectrum of the former molecule is induced under the chiral asymmetric field of the latter molecule. By analyzing the magnitude of induced circular dichroism, it was intended to clarify the relative orientation and distance of these molecules. These methods were successfully applied to the inclusion phenomena of an achiral molecule into chiral hosts such as cyclodextrin.[11−14] This work is an initial example of applying the method to inorganic host materials.

## Experimental Section

**Materials and Sample Preparation.** Synthetic sodium saponite (Smecton, Kunimie Ind. Co., Japan) was used as a smectite clay mineral. Cation-exchange capacity is stated to be 0.80 mequiv $g^{-1}$. An average particle size was determined to be 0.2 $\mu$m previously.[15] A stock dispersion of the clay mineral was prepared by dispersing 0.25 g of the clay into 500 mL of deionized water under ultrasonic agitation for 1 h. $FeSO_4 \cdot 7H_2O$ and $Fe(ClO_4)_3 \cdot 6H_2O$ were purchased from Wako Pure Chemical Ind. Co., Japan, and used without further purification. 2,2′,2″-Terpyridyl (terpy) was purchased from Tokyo Kasei Ind. Co. The molar extinction coefficient of terpy was determined to be $1.60 \times 10^4$ at 295 nm. A reaction between Fe(II) and terpy was investigated by adding 10 $\mu$L of 0.01 M $FeSO_4 \cdot 7H_2O$ solution to 3 mL of either pure water or a clay dispersion and thereafter adding a 0.01 M terpy−methanol solution with a microsyringe.

L- and D-Cysteines were obtained from Wako Pure Chemical Ind. Co., Japan. A $2.0 \times 10^{-3}$ M cysteine solution was prepared by dissolving cysteine in an aqueous 0.05 M tris-buffer solution (sample A). A solution of $[Fe(terpy)](ClO_4)_3$ was prepared by

* To whom correspondence should be addressed. E-mail: yamagisi@eps.s.u-tokyo.ac.jp. Fax: +81-3-5841-4553.
† Hiroshima University.
‡ The University of Tokyo.
§ Japan Science and Technology Corporation.
⊥ Aist.

10.1021/jp022412v CCC: $25.00 
Published on Web 07/26/2003

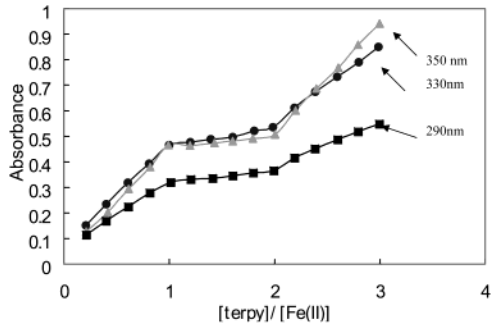


**Figure 1.** Dependence of adsorbance at 290 nm (■), 330 nm (●) and 350 nm (▲) when a methanol solution of terpy was added into an aqueous solution of $Fe(ClO_4)_2$. The concentration of $Fe(ClO_4)_2$ was $3.32 \times 10^{-5}$ M.

adding terpy in methanol into an aqueous solution of $Fe(ClO_4)_3$. A clay dispersion was added to an aqueous solution of [Fe(terpy)]$(ClO_4)_3$ and Δ-[Ni(phen)$_3$]$(ClO_4)_3$ (sample B). Sample B contained $5.0 \times 10^{-6}$ M [Fe(terpy)]$(ClO_4)_3$, $1.5 \times 10^{-5}$ M Δ-[Ni(phen)$_3$]$(ClO_4)_3$, and a $2.5 \times 10^{-3}$ equiv $L^{-1}$ clay. Oxidation of cysteine was monitored by the absorbance increase at 550 nm due to $[Fe(terpy)]^{2+}$ after mixing equal volumes of samples A and B. During experiments, solutions were bubbled with nitrogen gas.

**Instruments.** The UV−vis absorption spectrum of a sample solution or dispersion was measured with a UV−vis spectrometer, Shimadzu 105A (Shimadzu Ind. Co., Japan), at room temperature. Electric dichroism spectra were measured with an instrument as described previously.[15] The optical length of a cell was 10 mm. Electrodes were gold-coated copper. Electrode distance was 4.0 mm. The length and intensity of a square-shaped electric field pulse was changed from 1 to 10 ms and 0.2 to 2 kV. Monitoring light was polarized through a Gran-Thompson polarizer. Circular dichroism spectra were recorded with a spectropolarimeter J-700 (JASCO, Japan) at room temperature. A cell with the optical length of 10 cm was used throughout the experiments.

## Results and Discussion

**Electric Dichroism Measurements of $[Fe(terpy)]^{2+}$ Adsorbed by a Colloidal Clay in the Absence or Presence of $[Ni(phen)_3]^{2+}$.** Figure 1 shows the dependence of absorbance at three different wavelengths (290, 330, and 350 nm) when a methanol solution of terpy was added into an aqueous solution of $Fe(ClO_4)_2$. Clear inflection points were observed at the molecular ratios of [terpy]/[$Fe(ClO_4)_2$] = 1 and 2, confirming the successive formation of 1:1 and 1:2 complexes, or $[Fe(terpy)]^{2+}$ and $[Fe(terpy)_2]^{2+}$, respectively. Figure 2 shows the electronic absorption spectra of $[Fe(terpy)]^{2+}$ and $[Fe(terpy)_2]^{2+}$. The figure also includes the absorption spectrum of Δ-$[Ni(phen)_3]^{2+}$, which was used as a coadsorbate in the succeeding section.

The electric dichorism spectra were measured on an aqueous dispersion of sodium saponite and [Fe(terpy)]$(ClO_4)_2$. Upper and lower panels in Figure 3 show the typical signals at 550 nm when the monitoring light was polarized in parallel with or perpendicular to an electric field, respectively. An electric field was imposed as a square pulse of 1 ms × 1.0 kV $cm^{-1}$. The amplitude of absorbance change was found to follow the expression for orientational dichroism:[16]

$$\Delta A/A = (\rho/6)(1 + 3\cos\theta) \qquad (1)$$

in which $\Delta A$, $A$, $\rho$, and $\theta$ represent absorbance change, absorbance, reduced linear dichroism, and an angle between the

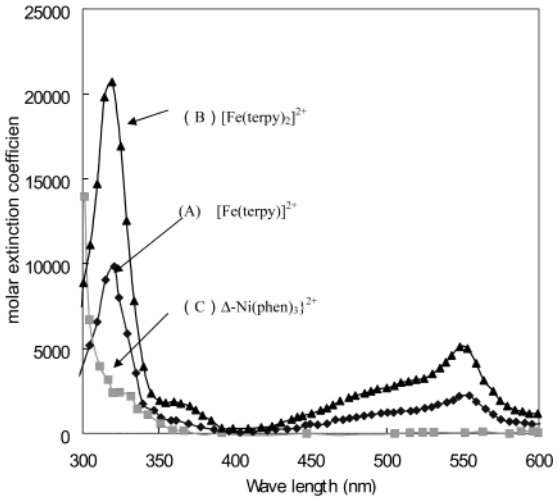


**Figure 2.** Electronic absorption spectra of $[Fe(terpy)]^{2+}$ (◆), $[Fe(terpy)_2]^{2+}$ (▲), and Δ-$[Ni(phen)_3]^{2+}$ (■).

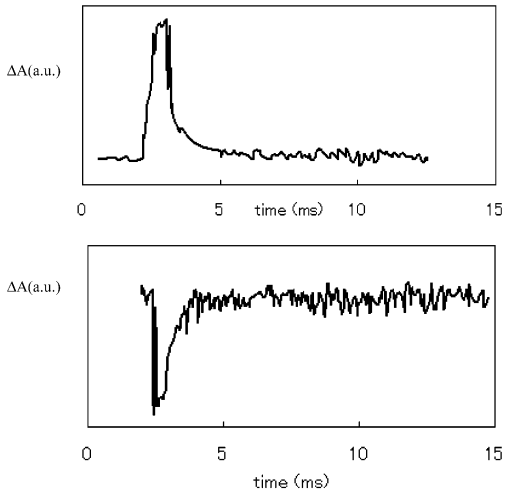


**Figure 3.** Examples of electric dichorism signals on an aqueous suspension of a clay ($2.0 \times 10^{-3}$ equiv $L^{-1}$) and $[Fe(terpy)]Cl_2$ ($2.50 \times 10^{-6}$ M). An angle between an electric field and the polarization of a monitoring light was 0° (upper) or 90° (lower). Wavelength was 550 nm.

polarization of monitoring light and an electric field, respectively. No dichroism was observed in the absence of sodium saponite. Thus the results indicated that the observed dichroism was due to $[Fe(terpy)]^{2+}$ ions bound to the clay particles orienting under an electric field.

When the transition moment of a molecule adsorbed on a clay surface makes an angle of $\phi$ with respect to a clay surface, the reduced linear dichroism is expressed as follows:[15]

$$\rho = -{}^3/_8(1 - 3\cos^2\phi)\Phi(\mathbf{E}) \qquad (2)$$

in which $\Phi(\mathbf{E})$ is a function representing the fraction of clay particles completely orienting in the direction of electric field. In deriving the above equation, it is assumed that the molecule orients in a random fashion at the fixed angle of $\phi$ on a clay surface. In the previous experiments, $\Phi(\mathbf{E})$ was determined to be 0.8 under the present electric field strength.[15]

Experiments were performed in the absence or presence of a coadsorbate, Δ-$[Ni(phen)_3]^{2+}$. The results are given in Figure 4, panels A and B, respectively. The transition moments at 470 and 550 nm were assumed to lie in the directions of the short and long axes of terpy ligands as shown in the inset of Figure 5. Based on this, the determined orientation of an $[Fe(terpy)]^{2+}$

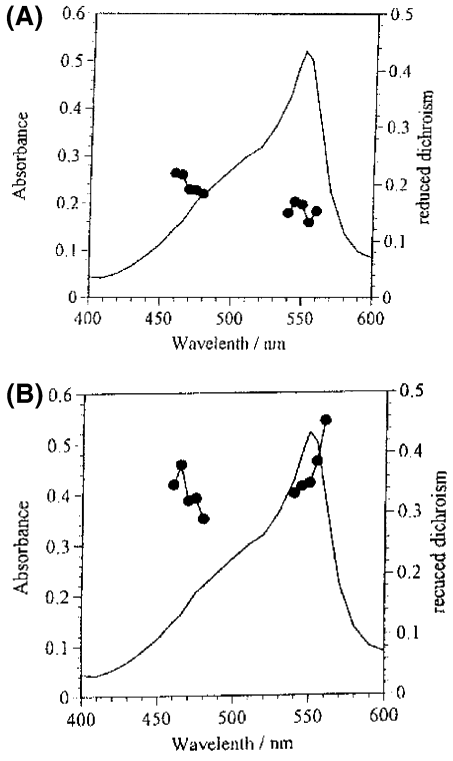


**Figure 4.** The magnitude of reduced electric dichorism due to [Fe(terpy)]$^{2+}$ adsorbed on a clay in the absence (A) or in the presence (B) of coadsorbed Δ-[Ni(phen)$_3$]$^{2+}$.

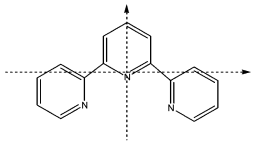

**Figure 5.** The directions of transition moments in [Fe(terpy)]$^{2+}$ at 470 and 550 nm.

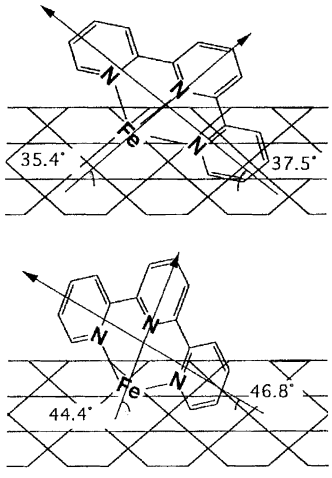


**Figure 6.** The orientation of an [Fe(terpy)]$^{2+}$ molecule adsorbed on a clay as determined by the electric dichroism measurements in the absence (upper) or in the presence (lower) of coadsorbed Δ-[Ni(phen)$_3$]$^{2+}$.

molecule is schematically shown in the upper and lower parts of Figure 6. The results imply that the [Fe(terpy)]$^{2+}$ molecule takes a more upright orientation when it coexists with Δ-[Ni(phen)$_3$]$^{2+}$ on a clay surface.

**Circular Dichroism Measurements of [Fe(terpy)]$^{2+}$ Adsorbed by a Colloidal Clay in the Presence of Chiral [Ni(phen)$_3$]$^{2+}$.** The interaction of [Fe(terpy)]$^{2+}$ with [Ni(phen)$_3$]$^{2+}$ on a clay surface was investigated by induced circular dichroism (CD). For that purpose, the CD spectrum of [Fe(terpy)]$^{2+}$ was measured in the presence of chiral [Ni(phen)$_3$]$^{2+}$. Figure 7 shows the CD spectrum when a clay was added to an aqueous solution of [Fe(terpy)](ClO$_4$)$_2$ and Δ-[Ni(phen)$_3$](ClO$_4$)$_2$ at various ratios. CD spectra were measured right after the addition of a clay. The absorption intensity was stable with time. With the increase of the concentration of Δ-[Ni(phen)$_3$](ClO$_4$)$_2$ at the constant concentrations of a clay and [Fe(terpy)](ClO$_4$)$_2$, the positive and negative peaks at 460 and 540 nm, respectively, were observed to increase. The intensities were saturated at the ratio of Δ-[Ni(phen)$_3$](ClO$_4$)$_2$/[Fe(terpy)](ClO$_4$)$_2$ = 2. The results indicated that these complexes were adsorbed at such close positions that the electronic transitions in [Fe(terpy)]$^{2+}$ were affected by the asymmetric field of Δ-[Ni(phen)$_3$]$^{2+}$.

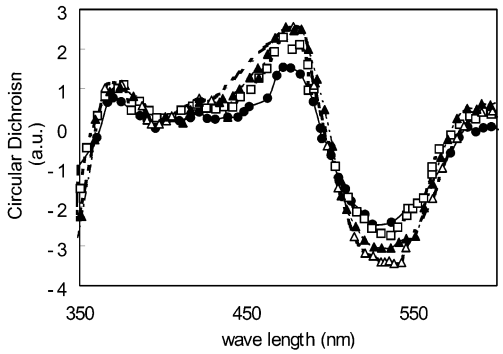


**Figure 7.** CD spectrum when a clay was added to an aqueous solution of [Fe(terpy)](ClO$_4$)$_2$ and Δ-[Ni(phen)$_3$](ClO$_4$)$_2$. The concentrations of clay and [Fe(terpy)](ClO$_4$)$_2$ were 2.0 × 10$^{-3}$ equiv L$^{-1}$ and 2.50 × 10$^{-6}$ M, respectively. The ratio of [Fe(terpy)](ClO$_4$)$_2$ to Δ-[Ni(phen)$_3$](ClO$_4$)$_2$ was varied from 1:1 to 3:1.

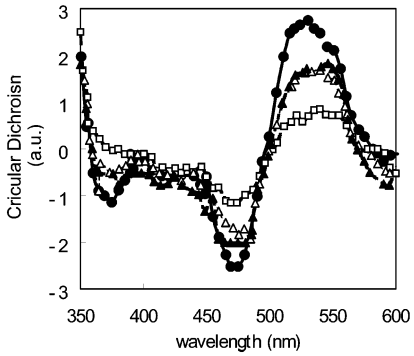


**Figure 8.** CD spectrum when Λ-[Ni(phen)$_3$](ClO$_4$)$_2$ was added to an aqueous solution of a clay and [Fe(terpy)](ClO$_4$)$_2$. The concentrations of a clay and [Fe(terpy)](ClO$_4$)$_2$ were 2.0 × 10$^{-3}$ equiv L$^{-1}$ and 2.50 × 10$^{-6}$ M, respectively. The ratio of [Fe(terpy)](ClO$_4$)$_2$ to Δ-[Ni(phen)$_3$](ClO$_4$)$_2$ was varied from 1:1 to 3:1.

Figure 8 shows the CD spectrum when Λ-[Ni(phen)$_3$](ClO$_4$)$_2$ was added to an aqueous dispersion of [Fe(terpy)]$^{2+}$ that had been already adsorbed by a colloidal clay. The negative and positive peaks were observed at 460 and 540 nm, respectively, which were opposite in sign in comparison to the results in Figure 7. This was an evidence that the induced CD was due to the molecular asymmetry of [Ni(phen)$_3$]$^{2+}$. The intensities of these peaks increased with time until it was saturated after 10 min. The results indicated that the adsorption and rearrangement of these two kinds of metal complexes on a clay surface were complete within this time. The final intensities were less than when a clay was added to an aqueous solution of [Fe(terpy)](ClO$_4$)$_2$ and Λ-[Ni(phen)$_3$](ClO$_4$)$_2$ as in the case of Figure 7. These results implied that the final arrangement of these metal complexes was dependent on the way of mixing. It should be

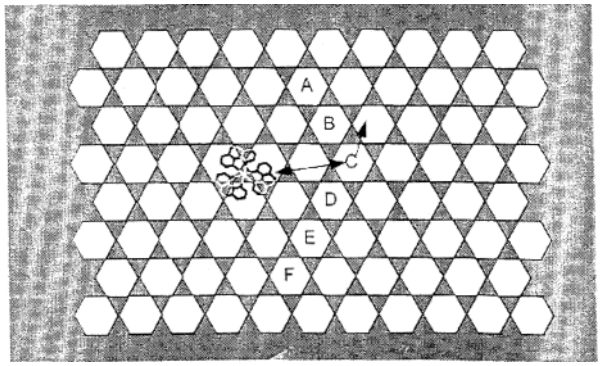


**Figure 9.** The model of coadsorption of $[Fe(terpy)]^{2+}$ and Δ-$[Ni(phen)_3]^{2+}$. Δ-$[Ni(phen)_3]^{2+}$ was placed as shown in the figure. $[Fe(terpy)]^{2+}$ was placed at any one of six positions as indicated by A−F.

noted that the above experiments were always performed under the conditions that the total amounts of these metal complexes were less than 1% of the cation-exchange capacity (CEC) of a clay. In other words, there is a tendency that these metal complexes aggregate on a clay surface even when there are sufficient adsorption sites for added metal complexes. Such aggregation might take place due to the hydrophobic interaction of polypyridyl ligands in these metal complexes.

**Interpretation of Induced Circular Dichroism on the Basis of Kirkwood−Tinoco Theory.** According to the theory on induced circular dichroism by Kirkwood and Tinoco,[17] optical rotatory power ($R_{0a}$) in the transition moment of an achiral molecule was caused by the dipole−dipole interaction of a chiral molecule. Such an effect is expressed by

$$R_{0a} = \pi\nu_a\mu_{0a}^2\sum\{\nu_{0j}^2(\alpha_{33} - \alpha_{11})(GF)_j\}/\{c(\nu_{0j}^2 - \nu_a^2)\} \quad (3)$$

$$(GF)_j = (1/r^3)[(\mathbf{e}_{0a}\cdot\mathbf{e}_j) - 3(\mathbf{e}_{0a}\cdot\mathbf{r}_j)(\mathbf{e}_j\cdot\mathbf{r}_j)]\mathbf{e}_{0a} \times \mathbf{e}_j\cdot\mathbf{r}_j \quad (4)$$

in which $R_{0a}$ is optical rotatory power for the transition from the ground state (0) to the excited state (a) of an achiral molecule, $\nu_a$ is the transition frequency, $\mu_{0a}$ is the transition moment, $\nu_{0j}$ is the frequency of transition from the ground state to the $j$th exited state of the chiral molecule, and $\alpha_{33}$ and $\alpha_{11}$ are the polarizability tensors. $(GF)_j$ is an orientational factor depending on the relative orientation between two transition moments due to chiral and achiral molecules. In the expression of $(GF)_j$ ( eq 4), $\mathbf{e}_{0a}$ is the unit vector of transition moment due to an achiral molecule ($\mu_{0a}$), $\mathbf{e}_j$ is the unit vector of transition moment due to a chiral molecule ($\mu_{0j}$), $\mathbf{r}$ is the positional vector from the center of an achiral molecule to the center of a chiral molecule, and $\mathbf{r}_j$ is the positional vector from the center of a chiral molecule to the center of transition moment $\mu_{0j}$. The summation is done over all of the transition moments due to a chiral molecule.

To apply the above equation to the present system, Δ-$[Ni(phen)_3]^{2+}$ was placed at an arbitrary position on a silicate surface. The orientation of this molecule was fixed with its $C_3$ axis perpendicular to the surface. Under this configuration, three bottoms of the 1,10-phenanthroline ligands of Δ-$[Ni(phen)_3]^{2+}$ were placed nearly at the center of the neighboring hexagonal holes. This configuration was found to be most stable by the previous theoretical simulation.[8−9] $[Fe(terpy)]^{2+}$ was placed at the neighborhood of Δ-$[Ni(phen)_3]^{2+}$ under the configuration as determined by the electric dichroism measurements (Figure 6B). Six positions were selected for the location of $[Fe(terpy)]^{2+}$ as indicated by A−F in Figure 9. For the calculation of $(GF)_j$, two transition moments ($\mu_{0a}$'s) were selected for $[Fe(terpy)]^{2+}$;

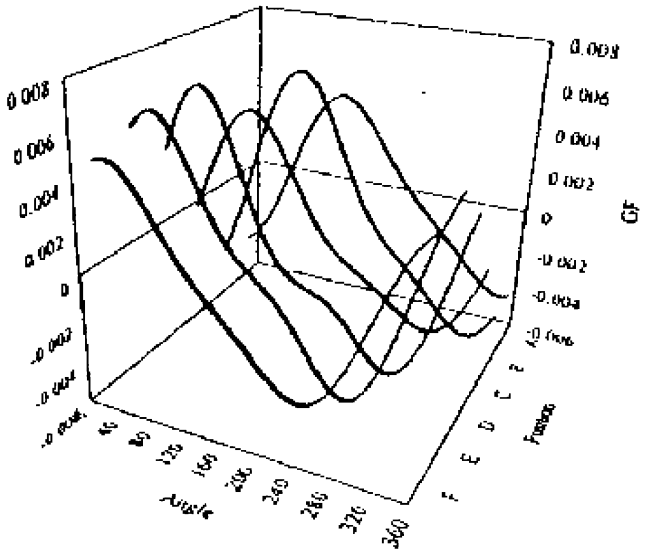


**Figure 10.** Results of calculation for $(GF)_j$ in eq 4 for the transition moment at 460 nm. $[Fe(terpy)]^{2+}$ was assumed to be located at any one of six selected positions (A−F). At each position, $(GF)_j$ is plotted as a function of rotation angle when $[Fe(terpy)]^{2+}$ was rotated under the configuration as shown in Figure 6B. Nearly the same results are obtained for the transition moment at 540 nm (not shown).

one was along the long axis of a terpy ligand and the other along its short axis. These transitions corresponded to the peaks at 460 and 540 nm in the electronic spectrum, respectively. Three transition moments were selected for Δ-$[Ni(phen)_3]^{2+}$, each of which was along the long axis of a coordinated 1,10-phenanthroline ligand. The transition moments along the short axis of the ligands were not taken into consideration because they formed no helical conformations. $(GF)_j$ in eq 4 was calculated by rotating $[Fe(terpy)]^{2+}$ on a clay surface under the fixed orientation (Figure 6B). The value of rotational angle (α) was taken to be zero where the long axis of terpy orients in the direction of the *b*-axis of a silicate sheet.

Figure 10 shows the results of calculation of $(GF)_j$ for the transition moment due to $[Fe(terpy)]^{2+}$ at 460 nm. Calculation was made at each of locations A−F in Figure 9 by changing the value of α from 0° to 360°. According to the calculation, $(GF)_j$ changes its sign from positive value to negative one around 120°−160° for all of the six selected positions. Nearly the same results were obtained for the transition moment at 540 nm. In other words, $(GF)_j$ is predicted to take the same sign for these two transitions at any value of α. The sign of $(GF)_j$ is considered to coincide with the sign of the circular dichroism spectrum. The above results were not consistent with the observed induced circular dichroism spectra, because they exhibit the opposite signs of the absorption peaks at 460 and 540 nm (Figure 7). At present, it is not possible to rationalize the discrepancy between the experimental results and the calculation results. One possibility is that the dipole−dipole interaction was not a sole factor inducing circular dichroism but some electronic interaction between these two complexes contributed a great deal. As far as we know, however, there is no theory taking into account such an electronic effect.

**Asymmetric Oxidation of Cysteine by $[Fe(terpy)]^{2+}$ on a Clay Surface.** With a purpose of examining the capability of chiral discrimination by a clay modified with a chiral molecule, the oxidation of cysteine by Fe(III) ions was investigated. An aqueous solution of either D- or L-cysteine was mixed with a dispersion of saponite that was ion-exchanged by $[Fe(terpy)]^{3+}$ and Δ-$[Ni(phen)_3]^{2+}$ as described in the Experimental Section.

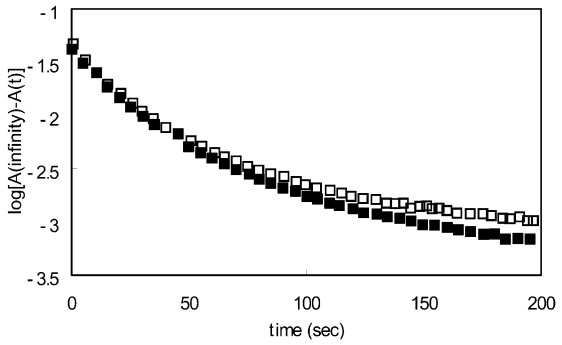


**Figure 11.** Dependence of $\log(A_t - A_\infty)$ on reaction time in which $A_t$ or $A_\infty$ is the absorbance at time $t$ or infinite time. Plots are for L-cysteine (□) and D-cysteine (■). The concentrations of cysteine, [Fe(terpy)]-$(ClO_4)_3$, Δ-[Ni(phen)$_3$]$(ClO_4)_3$, and a clay were $1.0 \times 10^{-3}$ M, $2.5 \times 10^{-6}$ M, $7.5 \times 10^{-6}$ M, and a $1.25 \times 10^{-3}$ equiv $L^{-1}$, respectively.

The reaction was monitored by the appearance of $[Fe(terpy)]^{2+}$ in terms of the absorbance increase at 550 nm.

Figure 11 shows the plot of $\log(A_t - A_\infty)$ versus time in which $A_t$ or $A_\infty$ is the absorbance at time $t$ or infinite time, respectively. The experiments were repeated three times. It was confirmed that L-cysteine was oxidized more rapidly than D-cycteine in the presence of the modified clay particles. Assuming that $[Fe(terpy)]^{3+}$ (or Fe(III)) reacts with cysteine (or RSH) in a bimolecular mechanism, the time change of [Fe(III)] is expressed as

$$-\mathrm{d[Fe(III)]}/\mathrm{d}t = k[\mathrm{Fe(III)}][\mathrm{RSH}] \quad (5)$$

or

$$[\mathrm{Fe(III)}] = [\mathrm{Fe(III)}]_0 \exp(-k[\mathrm{RSH}]) \quad (6)$$

in which it is assumed that the concentration of RSH is in large excess over the initial concentration of Fe(III), $[Fe(III)]_0$.

The plots in Figure 11 show that the dependence of $\log(A_t - A_\infty)$ on $t$ are not linear or the apparent bimolecular rate constant ($k$) changed with time. One possible reason for this would be that the adsorption state of $[Fe(terpy)]^{3+}$ on a clay surface was not homogeneous, in particular in connection with Δ-$[Ni(phen)_3]^{2+}$. Some would be adsorbed in an isolated site, while others would be surrounded by Δ-$[Ni(phen)_3]^{2+}$. Isolated $[Fe(terpy)]^{3+}$ ions might be more reactive in oxidizing cysteine than $[Fe(terpy)]^{3+}$ ions surrounded by Δ-$[Ni(phen)_3]^{2+}$. This might explain that the stereoselectivity in oxidation was more evident in the latter stage of the reaction as seen in the figure. By comparing the slopes of the curves in the time range of 100−200 s, it was concluded that the ratio of stereoselectivity or $k(\mathrm{L})/k(\mathrm{D})$ is estimated to be $1.3 \pm 0.1$. This selectivity is due to the steric control by the neighboring Δ-$[Ni(phen)_3]^{2+}$ ions.

## Conclusion

Interactions between $[Fe(terpy)]^{2+}$ and Δ-$[Ni(phen)_3]^{2+}$ on a clay surface were investigated by electric dichroism and circular dichroism measurements. As a result, the molecular orientation of adsorbed $[Fe(terpy)]^{2+}$ was affected by coadsorbed Δ-$[Ni(phen)_3]^{2+}$ and the circular dichroism was induced in the electronic spectrum of an achiral $[Fe(terpy)]^{2+}$. These results strongly suggest the presence of intermolecular interactions between these two kinds of molecules on a clay surface. Although interpretation of the induction of circular dichroism was attempted in terms of the Kirkwood−Tinoco theory, no consistent explanation was attained.

Stereoselectivity in the oxidation of cysteine by $[Fe(terpy)]^{3+}$ on a clay surface in the presence of a chiral metal complex, Δ-$[Ni(phen)_3]^{2+}$, is thought to be an evidence for the applicability of the clay minerals as a support for asymmetric induction.

**Acknowledgment.** This work was financially supported by a Grant-in-Aid for scientific Research on Priority Areas (417) from the Ministry of Education, Culture, Sports, Science and Technology (MEXT) of Japanese Government. This work has been supported by CREST of JST (Japan Science and Technology Corporation).

## References and Notes

(1) Brindley, G. W.; Brown, G. *Crystal Structures of Clay Minerals and their X-ray Identification;* Mineralogical Society: London, 1980.
(2) Umemura, Y.; Yamagishi, A.; Schoonheydt, R.; Persoons, A.; De Schryver, F. *J. Am. Chem. Soc.* **2002**, *124*, 992.
(3) Szabo, A.; Gournis, D.; Karakassides, M. A.; Petridis, D. *Chem. Mater*. **1998**, *10*, 639.
(4) Taniguchi, M.; Yamagishi, A.; Iwamoto, T. *Inorg. Chem.* **1991**, *30*, 2462.
(5) Yamagishi, A.; Taniguchi, M.; Takahashi, M.; Asada, C.; Matsushita, N.; Sato, H. *J. Phys. Chem.* **1994**, *98*, 7555.
(6) Yamagishi, A.; Taniguchi, M.; Imamura Y.; Sato, H. *Appl. Clay Sci.* **1996**, *11*, 1
(7) Yamagishi, A. In *Dynamic Processes on Solid Surfaces*; Tamaru, K., Ed.; Plunum Press: New York, 1993; Chapter 12.
(8) Sato, H.; Yamagishi, M.; Kato, S. *J. Am. Chem. Soc*. **1992**, *114*, 10934.
(9) Sato, H.; Yamagishi, A.; Naka, K.; Kato, S. *J. Phys. Chem.* **1996**, *100*, 1711.
(10) Moore, D. M.; Reynoleds, R. C., Jr. *X-ray Diffraction and the Identification and Analysis of Clay Minerals*; Oxford University Press: Oxford, U.K., 1989.
(11) Hesek, D.; Hembury, A. G.; Drew, M. G. B.; Borovkov, V. V.; Inoue Y. *J. Am. Chem. Soc*. **2001**, *123*, 12232.
(12) Kodaka, M. *J. Phys. Chem. A* **1998**, *102*, 8101.
(13) Murphy, R. S.; Barrons, T. C.; Mayer, B.; Marconi, G..; Bohne C. *J. Phys. Chem. A* **1999**, *103*, 137.
(14) Bortolus, P.; Marconi G..; Monti, S.; Mayer B. *J. Phys. Chem. A* **2002**, *106*, 1686.
(15) Nakamura, Y.; Yamagishi, A.; Iwamoto, T.; Koga, M.; *Clays Clay Miner.* **1988**, *36*, 530.
(16) Fredericq, E.; Houssier, C. *Electric Dichroism and Electric Birefringence*; Clarendon Press: Oxford, U.K., 1973.
(17) Tinoco, I., Jr. *Adv. Chem. Phys*. **1962**, *4* 113.